Received: 6 July 2023 | Revised: 9 August 2023 | Accepted: 10 August 2023 | Published online: 11 August 2023

REVIEW

Archives of Advanced Engineering Science
2023, Vol. 1(1) 2–10
DOI: 10.47852/bonviewAAES32021329
BON VIEW PUBLISHING

Tire Wear and Pollutants: An Overview of Research

Alfonse Ly[1,*] **and Zeinab El-Sayegh**[1]

[1]*Department of Automotive and Mechatronics Engineering, Ontario Tech University, Canada*

Abstract: Tire Road and Wear Particles are a major source of microplastic emissions. Tire and Road Wear Particles are important to study and understand as there are alarming amounts found in various environments. Currently, Tire and Road Wear Particles compared to other microplastics are not studied as rigorously in literature but are becoming a larger field of study due to their impact on emissions control. Tire Road and Wear Particles are commonly found as Styrene Butadiene Rubber, Butadiene Rubber, and Natural Rubber. To understand and quantify tire wear, experimental and mathematical models are developed to estimate tire wear. Tire wear can be measured experimentally using semi-empirical models, predetermined data, and sensor technologies. Tire wear is also measured mathematically using different modeling approaches and different friction models. This review discusses different and popular methodologies for estimating tire wear through experimental and simulated environments and furthermore discusses a review of the literature regarding tire wear emissions and its impact on the environment. Finally, it is evident that an accurate simulated tire wear model can be developed in the future alongside a driver model to predict tire wear emissions.

Keywords: tire, wear, TRWPs, emissions, pollutants, theoretical modeling, experimental modeling

1. Introduction

According to recent statistics, there are approximately 1.4 billion ground vehicles today including passenger vehicles, trucks, buses, and motorcycles (OICA, 2021). The majority of these vehicles are equipped with pneumatic tires that are worn over time as they roll over different surfaces and varying operating conditions. In 2020, it is estimated that there are up to 5,917,518 t/a of tire wear emissions globally and up to 2.6 kg/capita per year in Europe alone (Baensch-Baltruschat et al., 2020). The alarming climate crisis occurring globally has incentivized research on methods to estimate and reduce harmful emissions, including those given off by vehicles and tires. There are many initiatives and challenges sponsored by industry leaders and government associations to reduce harmful tire emissions such as the 'Plastics Challenge: Mitigating the Release of Microplastics from Tire Wear' from Innovation, Science and Economics Development Canada.

To understand the effects of tire wear emissions, commonly referred to as Tire Road and Wear Particles (TRWPs), the particulates must be estimated or measured (Baensch-Baltruschat et al., 2020). Currently, there are two methodologies to approximate tire wear emissions. The first method estimates tire wear emissions through emissions factors, such as observing the mass of tire wear and average mileage. The second method estimates tire wear by measuring tire mass loss from friction and abrasion. A deeper understanding of how tire wear is estimated and measured through modeling, and experimental methods can benefit in creating more accurate models in their respective categories or developing more comprehensive hybrid models (Khaleghian et al., 2017). In other tribology studies, surface texturing of the tire can be used as a method to control topography and friction at the tire-terrain contact. Surface texturing to control friction through tire topology has been a prominent research topic in the past 60 years (Costa et al., 2022). By controlling the surface texturing of the tire, it may be possible to retain adhesion to the terrain but reduce the amount of material expelled as emissions.

In the present day, reducing harmful emissions has been a priority on a global scale. Understanding tire wear and methods to measure/estimate the quantity of harmful emissions is critical to formulating strategies for mitigating the release of TRWPs (Environment and Climate Change Canada, 2022; US Environmental Protection Agency, 2023).

This study aims to present a technical survey on approaches to estimating tire wear through experimental and modeling approaches, the methods of measuring tire wear pollutants, and the effects of tire wear pollutants on the environment. Currently, there is a lack of literature in regard to tire wear research, especially detailed wear models linking to accurate emission values. The simulated and experimental tire wear models shown in this review are methodologies to estimate wear rate; however, they may not show the emissions of the tire wear and its impact on the environment. Wear emissions and factors are separately discussed further in the consequent section.

2. Tire Parameters

Preliminarily, before understanding different methodologies to measure and estimate tire wear, fundamental tire parameters should be established. This section provides an overview of important tire forces and moments.

*Corresponding author: Alfonse Ly, Department of Automotive and Mechatronics Engineering, Ontario Tech University, Canada. Email: alfonse.ly@ontariotechu.net

Figure 1
Free body diagram with tire forces and moments and angles in all three axes (Wong, 2022)

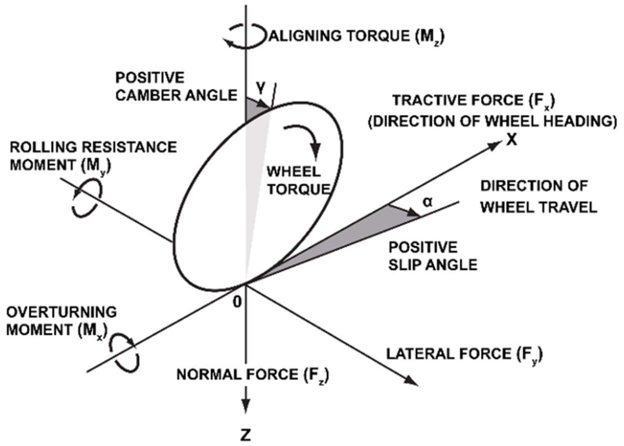

Figure 1 depicts the forces and moments that a tire may experience during operation according to SAE J670 JAN2008 (Wong, 2022). Moreover, these forces are also referred to as tire-terrain interaction characteristics as they are only present when the tire is in contact with a surface. Here, the tire is torqued in the longitudinal direction, and hence, F_x is a tractive force which is also commonly referred to as a more general term, the longitudinal force (Khaleghian et al., 2017; Environment and Climate Change Canada, 2022; US Environmental Protection Agency, 2023). Alternatively, for a free-rolling tire, the rolling resistance force can be seen in the opposite direction of the wheel heading in Figure 2. The longitudinal force is quantified through the tire rolling or sliding over a terrain. F_y is the lateral experienced by the tire during a cornering maneuver. The lateral force occurs when there is a difference in the direction of the wheel heading and travel. The angle about the tire center of this difference is the slip angle. In practical terms, a lateral force arises when a vehicle performs a cornering maneuver or experiences external lateral forces like crosswind. Lateral forces are considered a dynamic characteristic as it is directly proportional to the vehicle's lateral acceleration. F_z is the normal or vertical force that is also equivalent to the load experienced on the tire during regular

Figure 2
Free-body diagram of a free-rolling tire undergoing a cornering maneuver with a slip angle α

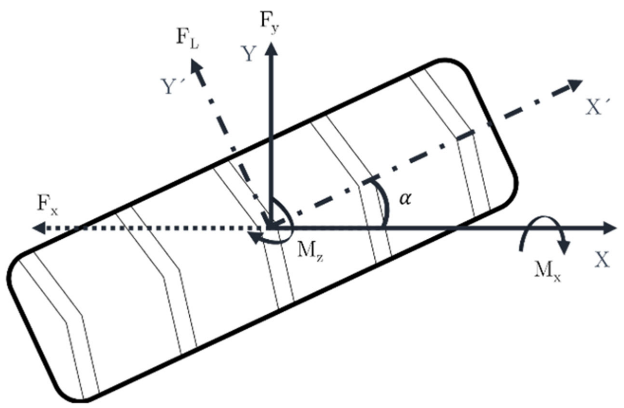

operations. M_x is the overturning moment which is produced due to surface irregularities and tire cambering. The overturning moment is present due to the uneven distribution of vertical pressure throughout the tire width on the contact patch and creates a torque about the longitudinal direction. M_y is the rolling resistance moment in the case of a free-rolling tire and is the torque in the case of a driven tire. The rolling resistance moment occurs as there are more vertical forces near the leading edge of the tire, which torques against the tire's rolling direction. M_z is the aligning moment which occurs during cornering maneuvers and is generally equivalent to the slip angle of the tire. The self-aligning moment is a function of the pneumatic trail and is highly dependent on the contact patch and tread contact with the surface. The pneumatic trail is present due to cornering forces. The cornering force is behind the applied side force, and the difference between the two applied forces is the pneumatic trail. This difference generates a torque that tends to realign the tire in the direction of motion (Doumiati et al., 2012; Gheshlaghi et al., 2022; Rajamani, 2011; Wong, 2022).

According to longitudinal vehicle dynamics, the normalized traction force for a tire, ρ, can be defined as (Rajamani, 2011):

$$\rho = \frac{\sqrt{F_x^2 + F_y^2}}{F_x} \tag{1}$$

where the peak quantity of this normalized traction force is called the friction coefficient, μ. While all the discussed tire parameters play a role in tire wear models, the wear models discussed in this review focus on frictional forces including F_x and F_y. Where many derivations for energy dissipation are relative to these frictional forces and their consequent dependent variables such as slip angle, α.

3. Experimental Tire Wear Modeling

Experimental-based methodologies to estimate tire wear involve quantitative measuring tools such as sensor data. The data are used to then relate to tire-road frictional data to estimate a wear model. Khaleghian et al. (2017) describe the experimental approach in three steps: obtaining wear-related parameters, correlating the data through wear-related formulations, and estimating the tire wear.

In 2002, Grosch (2004) developed an abrasion testing machine for empirical tire wear simulations. Grosch's experimental procedure uses a sample piece of a tire attached to a mount that rolls over an abrasive disc. As seen in Figure 3, this machine is titled the Grosch machine or the Laboratory Abrasion and Skid Tester (LAT) 100. In this test, the lateral force at a given slip angle is observed. In Grosch's analysis, tire wear was quantified as a function of abrasion, lateral force, and speed. Abrasion is defined as energy dissipation in the contact area of the wheel as seen in below:

$$A = A_{uo}\left(\frac{U}{U_{uo}}\right)^n \tag{2}$$

where abrasion, A, is a function of A_{uo}, the abrasion energy loss/dissipation of the compound at reference energy U_{uo} at experimentally set speed and n, the power index that is dependent on the tread and disc interaction. The energy dissipation U is determined by the tire's lateral force and predetermined slip angle as in the equation below:

$$U = F \cdot \sin\alpha \tag{3}$$

where F is the lateral force at a given slip angle, α. Abrasion was also formulated as a function of tire speed to analyze the wear at various operating conditions.

Figure 3
Schematic of the Grosch's LAT 100 tire abrasion machine used to evaluate the tire wear rate (Grosch, 2004)

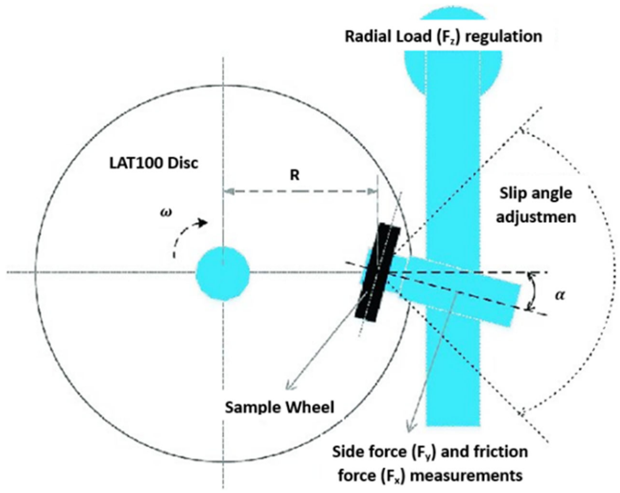

The equation below shows the abrasion, A, relative to A_{uo} , the abrasion energy dissipation of the compound at reference speed v_{uo}, and the experimentally set energy dissipation level relative to slip angle and load, m (Grosch, 2004).

$$A = A_{uo} \left(\frac{v}{v_{uo}} \right)^m \tag{4}$$

Grosch's studies showed that the LAT100 can determine wear rate factors comparable to real road tire wear data under limited conditions. Although the experimental datesets were in agreement with empirical tire datasets, the experimental conditions in which wear was tested on the machine were within a very finite range. This analysis used a small sample piece of tire that was not inflated, and therefore, the damping characteristics of a pneumatic tire were not included. Furthermore, the operating conditions were limited to small slip angles and low energy dissipation. However, this machine is advantageous as it can output many wear-related parameters in a short amount of time and was validated against limited real tire datasets.

In 2015, Ivanov et al. (2015) conducted a tire wear study by looking at the wear of rivets embedded into a truck tire. In this study, button head rivets were embedded along the width of a truck tire as seen in Figure 4.

The embedded rivets were weighed before the experimental procedure began and then once again post-experiment. The difference in weight was how this study analyzed the wearing along the width of the tire. In the experiment, the tires were sliding across an asphalt surface pulled by a tractor in a straight motion. This study showed that the wearing was most prominent in the middle path of the tire where the peak wear rate was 30.1 mg/km for increasing inflation pressures. However, the rivets on the side paths had higher wear rates with lower inflation pressures. This study showed that the patterns of wear rate along the width were comparable to the wearing of a tire and , however, does not observe how much the tire material wears. Additionally, it was tested in braking conditions as the tire slides over the asphalt rather than a driven or rolling tire.

Another popular method of experimental tire wear modeling is analyzing the tire tread at the block level. In 2021, Wu et al. (2021) analyzed an aircraft tire on a block level by varying the draft angle and root radius of the tread block as seen in Figure 5. The machine in this study used a normal loading mechanism for the tire sample and a horizontal feeding mechanism for the concrete and asphalt terrain. The wear width was found to peak at 5.5 mm at lower draft angles.

Similarly in 2021, Hartung et al. (2021) also investigated the wearing of a tread block using a different mechanism. In this study, the sample tread was also pressed onto a test track and slid over the concrete terrain for a given velocity as seen in Figure 6.

The tread sample post-procedure was processed using image processing tools to compare rubber profiles to evaluate tire wear along the contact surface of the tread. These profiles were then compared with finite element analysis (FEA) models of the same tread block where the results aligned with the experimental quantities. At block level, the studies neglect damping effects that pneumatic tires inherently are equipped with as they are inflated with air. Additionally, these experimental tests are capable of estimating tire wear at particular conditions; however, it does not fully replicate a rolling or torqued tire as the tire tread slides across the terrain.

With the advances in sensor technology, many experimental tire wear studies have been conducted with the sensors attached to the tire carcass. Strain sensors are a popular tool to obtain tire forces within the carcass (Singh, 2016; Singh et al., 2019; Miyazaki, 2001). Singh (2016) has done numerous studies using strain sensors on the sidewalls of the tire to correlate normal load and sideslip angles with algorithms to measure tire wear. In 2001, Miyazaki (2001) used multiple strain sensors in the tire to measure tire forces and compared these forces to a reference dataset to estimate tire wear. Pressure sensors are also used in tire wear studies such as those conducted by Hillenmayer and Kuchler (2006). The pressure sensors were used to obtain a frequency response as the tire is driven over a surface. The distinct frequency response is then used to estimate the normal loading of the vehicle and determines the type of terrain the vehicle is rolling over which then predicts tire wear over the given surface.

4. Simulated Tire Wear Modeling

Simulated tire wear approaches are analysis of tire wear using theoretical, mathematical, or computer-aided simulated models. Da Silva et al. (2012) used a similar approach of formulating wear with abrasion like in Grosch's work, but theoretically in the form of the bicycle model. This tire wear model was an estimation using only considering steady-state cornering maneuvers and a 2-degree-of-freedom bicycle model. In this model, any lateral load transfer was negligible, and no tire suspension characteristics were considered. Additionally, the model is only valid for low lateral accelerations. In this study, Silva describes tire wear as a function of steady-state longitudinal and lateral dynamic responses. This can be seen in the equation below, where W is the rate of wear, Ab is the abrasion of the tire-terrain interaction, F_y is the lateral force, α is the slip angle, S is the distance traveled by the vehicle during a maneuver, F_N is the normal force, and F_{N0} is the reference normal force. This model depended on the bicycle model to estimate the lateral force and side slip angle (Miyazaki, 2001).

$$W \propto Ab \cdot F_y \alpha \, S \frac{F_N}{F_{N0}} = Ab \, C_\alpha \alpha^2 S \, \frac{F_N}{F_{N0}} \tag{5}$$

Similarly, Chen et al. (2018) estimated tire wear using a 3-degree-of-freedom non-linear vehicle dynamic model. Chen used a power function that required the fitting of vehicle dynamic experimental data. To obtain the data for fitting, Chen used a hydraulic wear test system and cement terrain. The bicycle model can be seen to be a popular method for theoretical estimates of tire wear with the

Figure 4
Rivet placement on truck tire used to determine the tire wear rate by Ivanov et al. (2015)

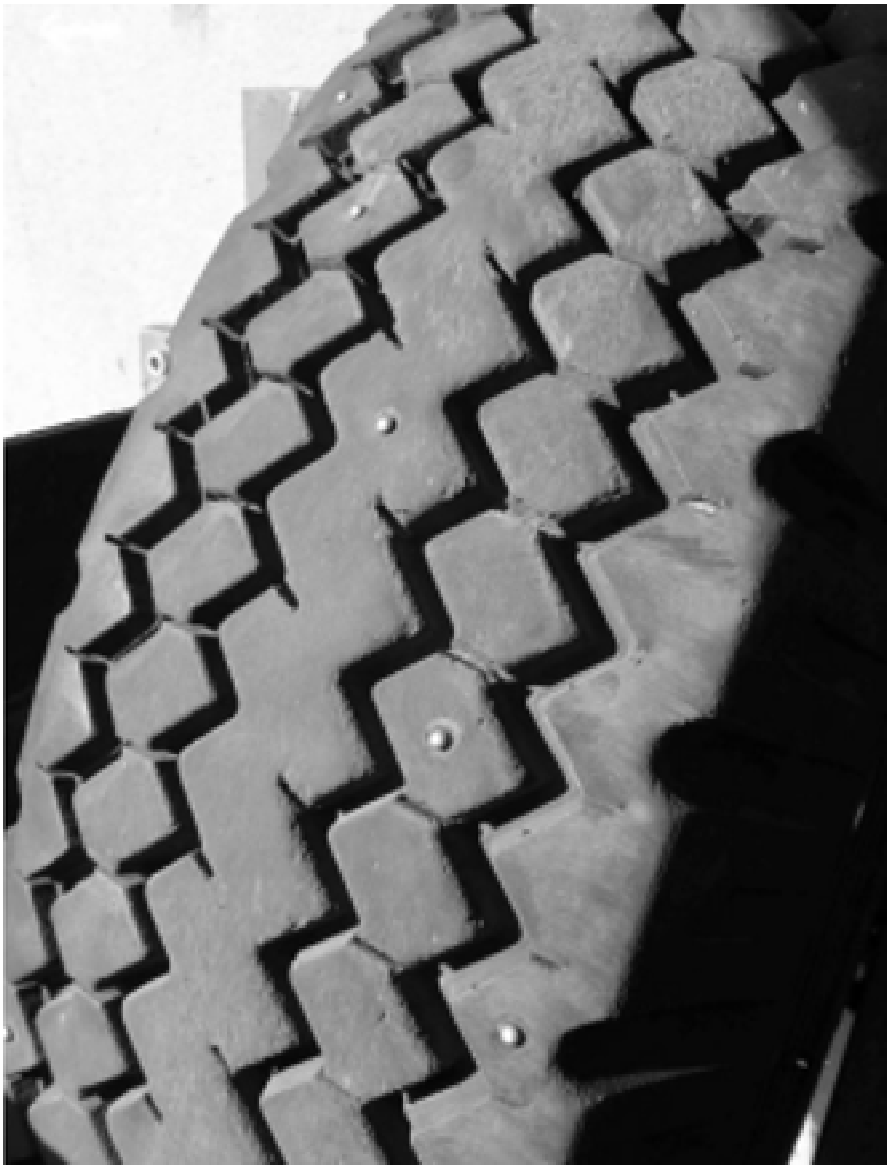

Figure 5
Schematic of a tire block diagram (Wu et al., 2021)

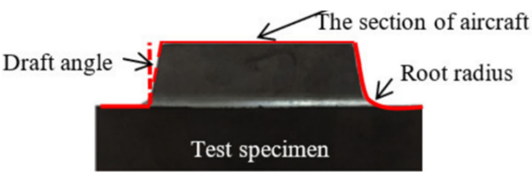

use of Kalman filters (Baffet et al., 2007; Baffet et al., 2008a; Baffet et al., 2008b; Chu et al., 2010a; Chu et al., 2010b; Pan et al., 2009; Zhu & Zheng, 2008; Zhang et al., 2009), where in many studies the Kalman filters are used to estimate side slip angles, cornering stiffnesses, yaw rates, speeds, and other tire forces derived from a bicycle model to analyze tire wear.

Figure 6
High-speed linear tester for friction and wear measurements (Hartung et al., 2021)

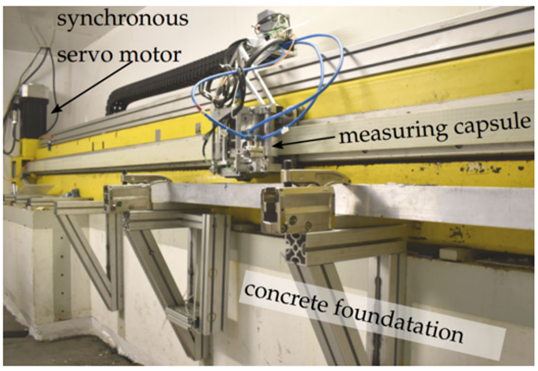

In 2021, Li et al. (2021) developed a tire wear model based on a large number of simulated datasets. In this study, vehicle dynamic responses to vertical load, longitudinal speeds, and inflation pressure were evaluated. These vehicle responses are converted to modal frequencies which are fed into a three-layer neural network. It should be noted that this tire wear model is assessed for limited conditions and under steady-state rolling simulations.

In 2011, Jin et al. (2011) developed an FEA tire wear model with a programmed subroutine using the Archard wear model. This model was a simple sliding abrasion relationship between two surfaces. This study analyzed the wear using Archard's wear model under straight free rolling and driven conditions and estimated tire wear as a function of mass and depth. In 2014, Zang et al. (2014) combine a FEA tire wear testing and neural network tools to estimate tire wear. In this study, an FEA tire model using the Neo-Hookean tread material equipped with constant shear and unconditional stability is used in several varying simulations. This analysis looks at a particular material type, and the neural network is trained for input variables of inflation pressure, speed, load, and different vibrational frequencies of the tire.

In 2022, Ly and El-Sayegh (2022) indirectly looked at the effects of tire wear using FEA. In this study, a truck tire with different groove numbers and tread depth to replicate the tire wearing to distinct levels was rolled over a given terrain at different operating conditions. This studied the rolling resistance coefficient of the tire at different tread depths over different moisture content soils. The FEA truck tire model for different tread depths of a 3-grooved tire can be seen in Figure 7. In this study, the truck tire is operating over varying sandy loam soils, and it was concluded that the quarter-depth groove has the highest rolling resistance coefficient with respect to vertical loading. The effect of groove depth was significantly visible at higher soil moisture content. For example, at 62% moist sandy loam, the quarter groove tire exhibited 12% more rolling resistance coefficient than the full-groove tire. The quarter groove tire model also exhibited a 3% more rolling resistance coefficient in comparison to the full-groove tire model at 10 km/h tire speed and 40 kN vertical load. Generally, the full-groove and half-groove tire models have similar rolling resistance coefficients. It was also concluded that the effect of tread depth is greater than that of the number of grooves on the rolling resistance coefficient.

Mathematical tire models are used to analyze the connections between a tire's forces and moments with slip angles. Many different tire models have been developed throughout the years to better understand vehicle dynamics and estimate vehicle dynamic properties. With this being said, popular tire models such as the brush model have been adapted with tire wear models to estimate tire wear. The brush model, as its namesake, analyzes the tire surface that is in contact with the terrain as bristles. Different regions in the contact surface experience different forces such as adhesion and friction forces. Three conventions are derived from the brush tire model: pure sideslip, pure longitudinal, and combined slipcases. Heinrich and Klüppel (2008) combined a hysteresis model with the brush model to analyze tire wear in an ABS braking

Figure 7
FEA tire wear simulation setup for 100%, 50%, and 25% groove depth truck tires (Ly & El-Sayegh, 2022)

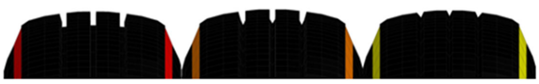

Figure 8
Parabolic pressure distribution in the contact region (Heinrich & Klüppel, 2008)

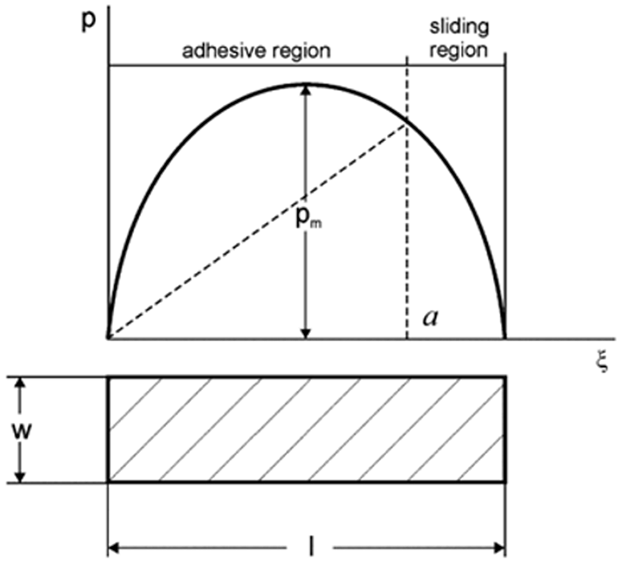

situation. Specifically, this study looks at the dependence of normal loading and kinetic friction coefficient in the contact area of slipping tires. With the brush model, in an ABS braking condition, the shear deformation was assumed to be visualized in a parabolic pressure distribution in the contact region as seen in Figure 8. Where ξ is the longitudinal displacement of a tire, l is the contact length of the tire tread, pm is the maximum value of contact pressure distribution and a is the breakaway point. Yamazaki et al. (1997) estimated tire friction similarly, however only using the partial sliding and pure sliding conventions of the brush model.

On a similar note, in 2022, Lu et al. (2022) developed a semi-empirical model using experimental values, tire footprint pressure distributions, and the brush model to estimate a tire block's wear. However, in 2011, Matilainen and Tuononen (2011), combined the brush model with the bicycle model to estimate tire wear friction. Specifically, the study looked at the potential friction the tire may encounter during a lateral driving maneuver using the bicycle model. Then using the tire forces acquired from the bicycle model to estimate friction using the brush model, however, assuming negligible tire stiffness.

5. Tire Road and Wear Particle Emissions

TRWPs are considered microplastics where the particles are smaller than 5 mm (Primpke et al., 2020). Compared to other microplastics, the literature in which TRWPs are studied as emissions is not studied rigorously (Khaleghian et al., 2017). However, due to alarming amounts of TRWPs found in different environments, the increase of studies regarding this topic has increased. In 2018, Gosmann et al., (2021) claimed that TRWPs contribute to over 50% of microplastic emissions in Denmark and Norway. Some studies show that TRWPs amount to the majority of microplastics found in some marine environments (Gosmann et al., 2021; Baensch-Baltruschat et al., 2020). TRWPs can be mostly found to be Styrene Butadiene Rubber (SBR), Butadiene Rubber (BR), and Natural Rubber (NR) (Wagner & Lambert, 2018). Where SBRs and BRs are mainly found in passenger car tire compositions and NRs in Truck tires (Jekel, 2019). Out of the

Figure 9
Tire road and particle wear categories based on morphology (Park et al., 2018)

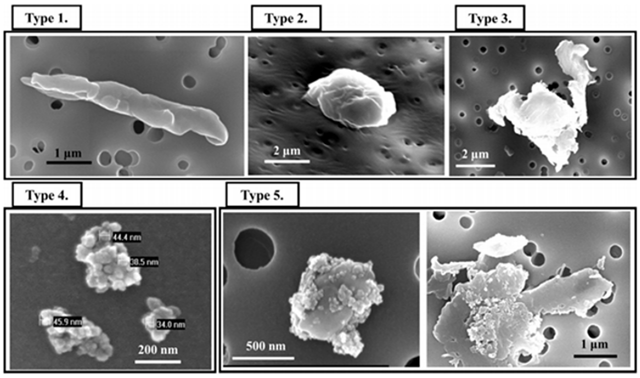

Figure 10
Car tire tread and truck tire tread contributions to tire road and particle wear (Heinrich & Klüppel, 2008)

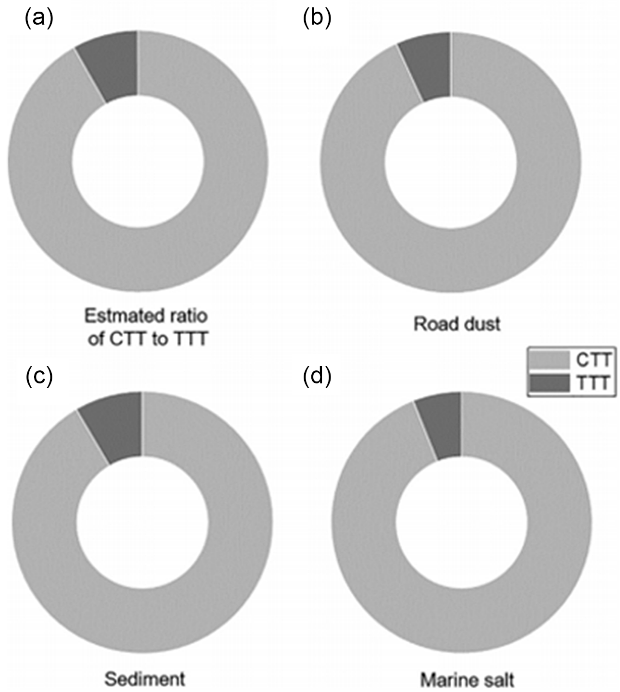

two types of TRWPs, NRs are known to be more wear and impact-resistant (Wagner et al., 2018). However, studies have also shown that truck tire wear emissions are a fraction of passenger car tire emissions at approximately a 1:11 ratio (Bertling et al., 2018; Gosmann et al., 2021).

Park et al. (2018) classified TRWPs into five distinct categories depending on the particle's geometry and size. This can be seen in Figure 9, where Type 1 particles are TRWPs in elongated tube shapes that are formed most commonly and are found at the tire-terrain contact. Type 2 particles are spherical in shape, averaged at around 2.5µ m. Type 1 and type 2 particles make up the majority of TRWPs compared to the five types in this study. The type 1 particle was seen to form into type 2 particles through secondary wear processes. Type 3 TRWPs are irregular in shape and are on average larger than type 1 and type 2. The study suggests that type 3 particles originate from severe tire-terrain contacts such as critical cornering or braking situations where much higher friction between tire and terrain is experienced. Type 4 and 5 particles are much smaller in size compared to the other types and are formed by combining or adhering with other larger particles.

The location in which TRWPs are concentrated can be variable as well, depending on roadways, waterways, and different paths the TRWPs may maintain location or move. That being said, studies do show that TRWPs can be mainly found in urban driving areas, compared to highway driving areas (Baensch-Baltruschat et al., 2021; Wik & Dave, 2009). The frequency of braking, accelerating, and encountering varying road characteristics are much higher on urban roads than on highways (Park et al., 2018). This being said, TRWP emissions can be categorized into three locations: ambient air, water, and soil. The emissions through air can be taken in by humans and animals through inhalation, or just into the nearby environment through deposition. Emissions into waters and soils can pose ecotoxicological risks or transport the TRWPs into different areas through runoffs. Some studies have estimated the origin of TRWPs found in road dust, sediment, and marine salt (Baensch-Baltruschat et al., 2021). One study shows that car tire tread contributes most of the TRWPs as seen in Figure 10, which is concurrent to that of some studies (Jekel, 2019; Wagner et al., 2018), where Car Tire Treads and Truck Tire Treads are CTTs and TTTs, respectively. Although different studies estimate the ratio differently between CTTs and TTTs, it is undoubtedly that CTTs output more TRWPs than emissions of the two.

Though present, TRWPs are not majorly found in ambient air where only 0.1-10% of TRWPs end up airborne (Baensch-Baltruschat et al., 2021; Stalnaker et al., 1996; Wik & Dave, 2009). Many TRWPs can be found in road dust and soils up to 210 g/kg dry weight (Kumata et al., 2000). It was found that there are more pollutants found within tunnels compared to outside tunnels due to the dilation of TRWPs outside of a concentrated area (Saito, 1989). Another study showed that there can be found up to 117 g/kg dry weight of TRWPs in soils close to automobile roads and can be seen to drop to below 80% of microplastic emissions at 30m away from the road (Boulter et al., 2006). TRWPs can also be found in sewage sludge that may be applied to agricultural soils. In 2003, Fjällborg and Dave (2003) estimated the number of TRWPs may end up in agricultural soils by extrapolating the zinc emissions from tires into agricultural sewage. In road runoffs and receiving waters, studies show that TRWPs can be found from 0.3 to 197 mg/l (Kumata et al., 2000).

Another study studied the TRWP concentration in five separate locations in runways and receiving waters through three stages of a storm. It was seen that there was two times less TRWP concentration in the receiving waters post-storm event indicating that the tire wear particles were flushed away from the initial concentration area (Kumata et al., 1997).

It was noted that estimating tire wear particles through chemical indicators and chemical sampling may be inaccurate to how much TRWPs are actually emitted through vehicles (Wagner et al., 2018). Capturing as many TRWPs in real time may provide a more accurate estimate of TRWPs emissions. As such, one study Park et al. (2018) looks at capturing the TRWPs within an enclosed space to look at the TRWP size, mass, and type as seen in Figure 11. Similarly, in 2021, Tonegawa and Sasaki (2021) developed an indoor tire wear tester and an on-road tire wear tester to compare results. The on-road tire wear tester can be seen in Figure 12, where a nozzle is placed behind the tire to suction the generated tire abrasion and dust. The particles were filtered to type 1 particles and other types to compare results with the control indoor test machine. It was found that for a constant

Figure 11
Enclosed tire road and wear particle capturing system (Park et al., 2018)

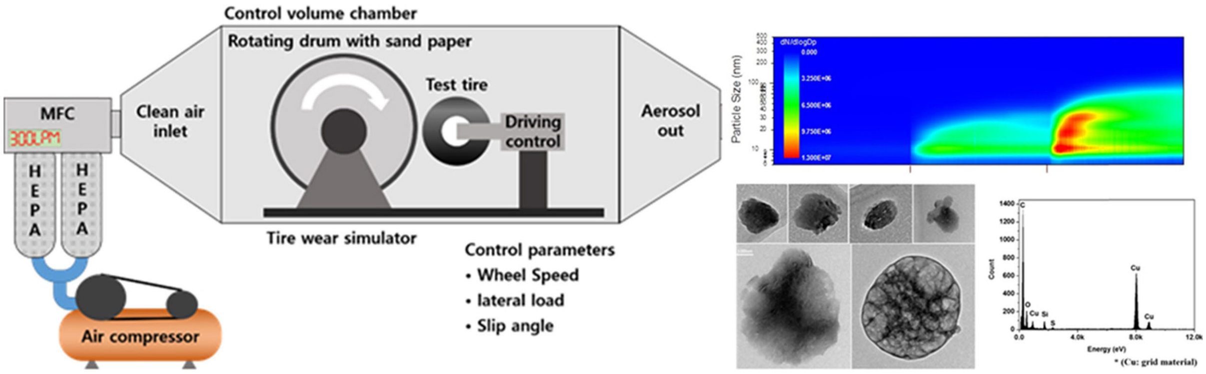

Figure 12
Enclosed tire road and particle wear capturing system (Tonegawa & Sasaki, 2021)

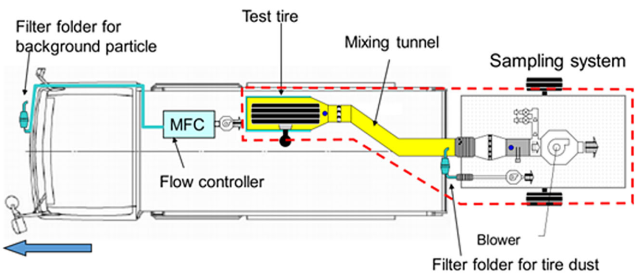

speed, the tire wear particles were similar in size; however at large lateral accelerations, the results were dramatically different.

6. Conclusion

In conclusion, tire wear particles are a significant source of microplastic emissions that have been found to contribute to over 50% of microplastic emissions in some countries. Tire wear particles are composed of various materials, including Styrene Butadiene rubber, Butadiene rubber, and natural rubber. The concentration of tire wear particles can vary depending on location, with urban driving areas having higher concentrations compared to highways. Tire wear particles can be found in ambient air, water, and soil, posing potential ecotoxicological risks. While estimating tire wear particle emissions through chemical indicators and sampling may be inaccurate, capturing tire wear particles in real time provides more accurate estimates. Developing solutions to mitigate tire wear particle emissions is necessary to reduce the impact of microplastic pollution on the environment and human health. Currently, there is much research developed in the field of the tire wearing through experimental methods, modeling methods, and semi-empirical methods. In literature, much experimental and modeling research is done on estimating tire wearing for dynamic and control problems through sensors and tests. These methods are accountable to estimate tire wear and , however, may have trouble extrapolating their results as tire wear particle emissions. To account for this, estimating tire wear particles can be done by looking at indicators and markers of the wear particles in surroundings such as soil, water, and roads. However, due to different environmental factors, it may be difficult to discern the exact origins of the particulate, whether they can be found in tires or other sources that are further away from automobile roads. Thus, it is important to continue research on estimating tire wear and methods of capturing tire wear to further reduce harmful emissions through tire wear particles. It can be seen that wear emissions estimated through trackers can be inaccurate, and experimental wear modeling can become expensive and time-consuming. Current simulated tire wear models in the literature are still simple and developed under limited operating conditions. Introspectively, a more optimized and capable tire model to simulate the tire wear model may be developed alongside a driver model in order to obtain a more accurate tire wear emissions value.

Acknowledgement

The authors would like to acknowledge Volvo Groups Trucks Technology and NSERC for their support during this project.

Conflicts of Interest

The authors declare that they have no conflicts of interest to this work.

References

Baensch-Baltruschat, B., Kocher, B., Kochleus, C., Stock, F., & Reifferscheid, G. (2021). Tyre and road wear particles - A calculation of generation, transport and release to water and soil with special regard to German roads. *Science of The Total Environment*, 752, https://doi.org/10.1016/j.scitotenv.2020.141939.

Baensch-Baltruschat, B., Kocher, B., Stock, F., & Reifferscheid, G. (2020). Tyre and road wear particles (TRWP)-A review of generation, properties, emissions, human health risk, ecotoxicity, and fate in the environment. *Science of the Total Environment*, *733*.

Baffet, G., Charara, A., & Dherbomez, G. (2007). An observer of tire–road forces and friction for active security vehicle systems. *IEEE/ASME Transactions on Mechatronics*, *12*(6), 651–661.

Baffet, G., Charara, A., & Lechner, D. (2008a). Estimation of tire-road forces and vehicle sideslip angle. In J. Arámburo-Lizárraga & A. Ramírez-Treviño (Eds.), *Advances in robotics, automation and control* (pp. 137–150). Books on Demand.

Baffet, G., Charara, A., Lechner, D., & Thomas, D. (2008b). Experimental evaluation of observers for tire–road forces, sideslip angle and wheel cornering stiffness. *Vehicle System Dynamics, 46*(6), 501–520.

Bertling, J., Bertling, R., & Hamann, L. (2018). *Kunststoffe in der umwelt: Mikro-und makroplastik*. German: Fraunhofer-Institut für Umwelt-, Sicherheits- und Energietechnik UMSICHT.

Boulter, P., Thorpe, A., Harrison, R., & Allen, A. (2006). *Road vehicle non-exhaust particulate matter: Final report on emission modelling*. UK: TRL Limited.

Chen, X., Xu, N., & Guo, K. (2018). Tire wear estimation based on nonlinear lateral dynamic of multi-axle steering vehicle. *International Journal of Automotive Technology*, *19*, 63–75.

Chu, L., Shi, Y., Zhang, Y., Liu, H., & Xu, M. (2010a). Vehicle lateral and longitudinal velocity estimation based on adaptive Kalman filter. In *2010 3rd International Conference on Advanced Computer Theory and Engineering*, *3*, 3–325.

Chu, L., Zhang, Y., Shi, Y., Xu, M., & Liu, M. (2010b). Vehicle lateral and longitudinal velocity estimation based on unscented Kalman filter. In *2010 2nd International Conference on Education Technology and Computer*, *3*, 3–427.

Costa, H. L., Schille, J., & Rosenkranz, A. (2022). Tailored surface textures to increase friction—A review. *Friction*, *10*(9), 1285–1304.

Da Silva, M., Cunha, R., & Neto, A. (2012). A simplified model for evaluating tire wear during conceptual design. *International Journal of Automotive Technology*, *13*, 915–922.

Doumiati, M., Charara, A., Victorino, A., & Lechner, D. (2012). *Vehicle dynamics estimation using Kalman filtering: Experimental validation*. USA: John Wiley & Sons.

Environment and Climate Change Canada (2022). Plastics challenge: Mitigating the release of microplastics from tire wear. Retrieved from: https://Ised-isde.Canada.Ca/,ised-isde.canada.ca/site/innovative-solutions-canada/en/plastics-challenge-mitigating-release-microplastics-tire-wear.

Fjällborg, B., & Dave, G. (2003). Toxicity of copper in sewage sludge. *Environment International*, *28*(8), 761–769.

Gheshlaghi, F., Rakheja, S., & El-Gindy, M. (2022). Tyre-terrain interaction modelling and analysis: Literature survey. *International Journal of Vehicle Systems Modelling and Testing, 16*(2), 113–149.

Gosmann, I., Halbach, M., & Scholz-Böttcher, B. M. (2021). Car and truck tire wear particles in complex environmental samples–A quantitative comparison with "traditional" microplastic polymer mass loads. *Science of the Total Environment, 773*.

Grosch, K. (2004). Correlation between road wear of tires and computer road wear simulation using laboratory abrasion data. *Rubber Chemistry and Technology*, *77*(5), 791–814.

Hartung, F., Garcia, M. A., Berger, T., Hindemith, M., Wangenheim, M., & Kaliske, M. (2021). Experimental and numerical investigation of tire tread wear on block level. *Lubricants*, *9*(12), 113.

Heinrich, G., & Klüppel, M. (2008). Rubber friction, tread deformation and tire traction. *Wear, 265*(7–8), 1052–1060.

Hillenmayer, F., & Kuchler, G. (2006). *System for monitoring a vehicle with pneumatic tires, signal analysis method, and vehicle tire*. USA: US Patent No. 7,000,462.

Ivanov, R., Georgiev, K., Kadikyanov, G., & Staneva, G. (2015). An experimental research on the wear of truck tire. *Transport Problems*, *10*.

Jekel, M. (2019). Scientific report on tyre and road wear particles, TRWP, in the aquatic environment. In *The European Tyre & Rubber Manufacturers Association*, 1–35.

Jin, C., Hou, C. Y., & Jin, X. X. (2011). Fe simulation of tire wear with complicated tread pattern. *Procedia Engineering, 15*, 5015–5019.

Khaleghian, S., Emami, A., & Taheri, S. (2017). A technical survey on tire-road friction estimation. *Friction, 5*, 123–146.

Kumata, H., Sanada, Y., Takada, H., & Ueno, T. (2000). Historical trends of n-cyclohexyl-2-benzothiazolamine, 2-(4-morpholinyl) benzothiazole, and other anthropogenic contaminants in the urban reservoir sediment core. *Environmental Science & Technology, 34*(2), 246–253.

Kumata, H., Takad, H., & Ogura, N. (1997). *2-(4-morpholinyl) benzothiazole as an indicator of tire-wear particles and road dust in the urban environment*. USA: ACS Publications.

Li, B., Quan, Z., Bei, S., Zhang, L., & Mao, H. (2021). An estimation algorithm for tire wear using intelligent tire concept. In *Proceedings of the Institution of Mechanical Engineers, Part D: Journal of Automobile Engineering*, *235*(10-11), 2712–2725.

Lu, L., Lu, D., Wu, H., Li, L., Wang, W., & Lyu, M. (2022). Research and modeling of tire cornering characteristics considering tread wear based on unitire model. In *Proceedings of the Institution of Mechanical Engineers, Part D: Journal of Automobile Engineering*, *236*(6), 1155–1169.

Ly, A., & El-Sayegh, Z. (2022). Effect of truck tire tread design on tire-terrain interaction using advanced computational techniques. *International Journal of Heavy Vehicle Systems*, *30*(3), 365–379.

Matilainen, M. J., & Tuononen, A. J. (2011). Tire friction potential estimation from measured tie rod forces. In *2011 IEEE Intelligent Vehicles Symposium (IV)*, 320–325.

Miyazaki, N. (2001). *Road surface friction sensor and road surface friction coefficient detector, and vehicle antilock braking device*. USA: US Patent. US20020120383A11.

OICA (2021). *World Motor Vehicle Production, by manufacturer and type*. Retrieved from: https://www.oica.net/category/vehicles-in-use/

Pan, Z., Zong, C., Zhang, J., Xie, X., & Dong, Y. (2009) UKF and EKF estimator design based on a nonlinear vehicle model containing unitire model. In *2009 International Conference on Mechatronics and Automation*, 4780–4784.

Park, I., Kim, H., & Lee, S. (2018). Characteristics of tire wear particles generated in a laboratory simulation of tire/road contact conditions. *Journal of Aerosol Science*, *124*, 30–40.

Primpke, S., Christiansen, S. H., Cowger, W., De Frond, H., Deshpande, A., Fischer, M., . . . , & Wiggin, K. J. (2020). Critical assessment of analytical methods for the harmonized and cost-efficient analysis of microplastics. *Applied Spectroscopy, 74*(9), 1012–1047.

Rajamani, R. (2011). *Vehicle dynamics and control*. German: Springer Science & Business Media.

Saito, T. (1989). Determination of styrene-butadiene and isoprene tire tread rubbers in piled particulate matter. *Journal of Analytical and Applied Pyrolysis, 15*, 227–235.

Singh, K. B. (2016). *Intelligent tire-based road friction estimation system and method*. USA: US Patent No. 9,340,211.

Singh, K. B., Arat, M. A., & Taheri, S. (2019). Literature review and fundamental approaches for vehicle and tire state estimation. *Vehicle System Dynamics, 57*(11), 1643–1665.

Stalnaker, D., Turner, J., Parekh, D., Whittle, B., & Norton, R. (1996). Indoor simulation of tire wear: Some case studies. *Tire Science and Technology*, *24*(2), 94–118.

Tonegawa, Y., & Sasaki, S. (2021). Development of tire-wear particle emission measurements for passenger vehicles.

Emission Control Science and Technology, 7(1), 56–62. https://doi.org/10.1007/s40825-020-00181-z

US Environmental Protection Agency (2023). *Where the rubber meets the road: Opportunities to address tire wear particles in waterways*. USA: US Environmental Protection Agency.

Wagner, M., & Lambert, S. (2018). *Freshwater microplastics: Emerging environmental contaminants*. German: Springer Nature.

Wagner, S., Huffer, T., Klockner, P., Wehrhahn, M., Hofmann, T., & Reemtsma, T. (2018). Tire wear particles in the aquatic environment-a review on generation, analysis, occurrence, fate and effects. *Water Research*, *139*, 83–100.

Wik, A., & Dave, G. (2009). Occurrence and effects of tire wear particles in the environment–A critical review and an initial risk assessment. *Environmental Pollution*, *157*(1), 1–11.

Wong, J. Y. (2022). *Theory of ground vehicles*. USA: John Wiley & Sons.

Wu, J., Chen, L., Chen, D., Wang, Y., Su, B., & Cui, Z. (2021). Experiment and simulation research on the fatigue wear of aircraft tire tread rubber. *Polymers*, *13*(7).

Yamazaki, S., Furukawa, O., & Suzuki, T. (1997). Study on real time estimation of tire to road friction. *Vehicle System Dynamics, 27*(S1), 225–233.

Zang, L., Zhao, Y., Li, B., Wang, J., & Du, X. (2014). Mechanical elastic wheel improving road holding and wear resistance of tire. *Transactions of the Chinese Society of Agricultural Engineering*, *30*(12), 56–63.

Zhang, W., Ding, N., Yu, G., & Zhou, W. (2009). Virtual sensors design in vehicle sideslip angle and velocity of the centre of gravity estimation. In *2009 9th International Conference on Electronic Measurement & Instruments*, 3–652.

Zhu, T., & Zheng, H. (2008). Application of unscented kalman filter to vehicle state estimation. In *2008 ISECS International Colloquium on Computing, Communication, Control, and Management*, *2*, 135–139.

How to Cite: Ly, A. & El-Sayegh, Z. (2023). Tire Wear and Pollutants: An Overview of Research. *Archives of Advanced Engineering Science* 1(1), 2–10, https://doi.org/10.47852/bonviewAAES32021329